Retraction

Retraction for "Odor maps in the olfactory cortex," by Zhihua Zou, Fusheng Li, and Linda B. Buck, which appeared in issue 21, May 24, 2005, of *Proc Natl Acad Sci USA* (102:7724–7729; first published May 23, 2005; 10.1073/pnas.0503027102).

The undersigned authors wish to note the following: "This article described patterns of c-Fos labeling in anterior piriform cortex following exposure of mice to odorants. In efforts to replicate this work, we have observed c-Fos in sparsely distributed neurons, as reported, but we have found no evidence for the reported finding that odorants induce related patterns of c-Fos labeling in the two hemispheres and in different individuals. Inconsistencies have also been found between several images shown in the paper and the original data. Because of these discrepancies, the undersigned authors are retracting the article. We sincerely apologize for any confusion it has caused."

<div style="text-align:right">

Fusheng Li
Linda B. Buck

</div>

RETRACTION

Odor maps in the olfactory cortex

Zhihua Zou*†, Fusheng Li‡, and Linda B. Buck*†§

*Howard Hughes Medical Institute and Divisions of †Basic Sciences and ‡Public Health Sciences, Fred Hutchinson Cancer Research Center, 1100 Fairview Avenue North, Seattle, WA 98109

In the olfactory system, environmental chemicals are deconstructed into neural signals and then reconstructed to form odor perceptions. Much has been learned about odor coding in the olfactory epithelium and bulb, but little is known about how odors are subsequently encoded in the cortex to yield diverse perceptions. Here, we report that the representation of odors by fixed glomeruli in the olfactory bulb is transformed in the cortex into highly distributed and multiplexed odor maps. In the mouse olfactory cortex, individual odorants are represented by subsets of sparsely distributed neurons. Different odorants elicit distinct, but partially overlapping, patterns that are strikingly similar among individuals. With increases in odorant concentration, the representations expand spatially and include additional cortical neurons. Structurally related odorants have highly related representations, suggesting an underlying logic to the mapping of odor identities in the cortex.

odorant receptor | smell

In the olfactory system, sensory signals generated in the nasal olfactory epithelium (OE) are relayed through the olfactory bulb (OB) to the olfactory cortex (OC), which, in turn, transmits information to higher cortical areas and limbic structures (1–5). Odorant detection in the mouse OE is mediated by ≈1,000 different odorant receptors (ORs) (6–13), each expressed by a different subset of olfactory sensory neurons (14). Neurons with the same OR are randomly scattered in one OE zone (15, 16), but their axons all converge in a few fixed glomeruli in the OB (17–20). In the OE, different odorants are detected, and thereby encoded, by different combinations of ORs (14, 20, 21). Consequently, the representation of an odorant in the OE is a dispersed ensemble of neurons (22), each expressing one component OR of its receptor code (14), whereas, in the OB, the odorant is represented by a fixed combination of glomeruli whose spatial arrangement is similar among individuals (23–27).

Although much has been learned about the encoding of odor identities in the OE and OB, relatively little is known about how olfactory information is organized in the cortex. Using a genetic transneuronal tracer, we previously found that input from one OR is targeted to several loose clusters of neurons at stereotyped locations in the OC (28). In sharp contrast to the OB, where signals derived from different ORs are segregated in different glomeruli and projection neurons (29–31), it seems that inputs from different ORs partially overlap in the OC and that single cortical neurons receive combinatorial inputs from multiple different ORs (28).

Given the complexity of OR inputs in the cortex and the combinatorial use of ORs in odor detection, it was impossible to predict how OR inputs might encode odor identities in the OC. At one extreme, signals from different ORs that detect the same odorant might be colocalized at a few specific cortical locations, producing a distinct spatial code for the odorant. At the other extreme, signals from the different ORs might be targeted to many different locations, resulting in a highly distributed odor code. Previous electrophysiological studies (32–38) have described odorant responses by individual OC neurons but have not examined the spatial patterning of OC odor responses.

Here, we investigated how odors are represented in the OC using awake, freely behaving mice. We focused on the anterior piriform cortex (APC), a major olfactory cortical area that showed distinct patterns of OR inputs in genetic tracing studies (28). To visualize odor responses in single cells across the entire APC, we used the transcription factor c-Fos as a neuronal activity marker (39–41). c-Fos is rapidly and transiently induced in many types of neurons in response to calcium influx caused by depolarization (42). Furthermore, patterns of c-Fos induction recapitulate patterns of neuronal activity in many brain areas, including auditory, visual, and somatosensory cortices (43–46). For example, deflection of one whisker induces c-Fos in a single barrel representing that whisker in rat somatosensory cortex (45, 46).

Using this approach, we found that single odorants activate distinct patterns of neurons in the APC. Each odorant activates a small subset of cortical neurons that are sparsely, but unevenly, distributed across a large area. Different odorants have different, but partially overlapping, APC representations, and these representations are remarkably similar among individuals. The representations are concentration-dependent and expand both numerically and spatially with increases in odorant concentration. Structurally related odorants elicit highly similar patterns of APC activation, hinting that there might be an underlying logic to the manner in which olfactory information is mapped onto the cortex.

Methods

Odor Exposure. Adult male and female C57BL/6J mice (The Jackson Laboratory) were exposed to odorants singly within a modified polycarbonate vacuum-desiccator (inside diameter 149 mm, overall height 206 mm; Scienceware, Bel-Art Products, Pequannock, NJ) equipped with a grid-work platform. Forced-air (50 liters/min) that was deodorized (purified) by passage through a column containing activated charcoal (Whatman) entered and exited the chamber through ports at its top and bottom, respectively. Each animal was exposed to purified air for 16 h and then to purified air bubbled through odorant dissolved in either distilled water or DMSO (dimethyl sulfoxide) or, as controls, to water or DMSO alone. Odorant exposure was twice for 2 min with 5 min between the exposures. The animal was then exposed to purified air for an additional hour before killing to permit maximum accumulation of c-Fos protein (23, 40).

Odorants were purchased from Sigma-Aldrich or were gifts from International Flavors and Fragrances (Union Beach, NJ). To approximate what might be encountered in the natural environment, odorant concentrations used initially were the lowest that the experimenter could detect in air exiting the exposure chamber: fructone, 0.29 M; orange flower ether, 0.06 M; 2,5-dimethylpyrazine, 0.926 M; vanillin, 0.658 M; w-pentadecalactone, 0.42 M; l-menthol, 1.84 M; and amyl cinnamic aldehyde, 0.247 M. A lower concentration was used for other

---

odorants: ethyl butyrate, 8.6 mM and 86 mM; 3-methyl-1-butanethiol, 95.9 μM; benzyl mercaptan, 8 mM; methylamine, 0.032 M and 0.32 M; coniferan, 4.7 mM; camphor, 13 mM; and androstenone, 0.367 mM.

Immunohistochemistry. Mice were anaesthetized and perfused with 4% paraformaldehyde, and their brains were sectioned (14 μm) as described (28). Sections were incubated with rabbit anti-c-Fos antibody (0.4 μg/ml, sc-52, Santa Cruz Biotechnology) for 2 h at 37°C, followed by biotinylated goat anti-rabbit antibody (0.8 μg/ml, Vector Laboratories) for 1 h at room temperature. Antibody binding was visualized using ABC (avidin-biotin complexes) elite and DAB (diaminobenzidine) kits from Vector Laboratories. The kits were used according to the manufacturer's instructions, with the nickel chloride enhancement option used in the case of the DAB kit.

Diagrams of c-Fos Labeling in the Piriform Cortex. Digital photographs of immunostained sections were examined by computer. The location of each c-Fos$^+$ neuron was confirmed by microscopy and marked with a blue dot on the digital image. The piriform cortex in each image was next divided into segments according to its curvature, and the blue dots were then aligned vertically between black dots marking the dorsal and ventral limits of the piriform cortex. These vertical representations of individual sections were then combined with their ventral limits aligned along the horizontal axis to show the dorsal–ventral locations of c-Fos$^+$ neurons from the rostral end (left) to the caudal end (right) of the APC.

In initial experiments, we immunostained all of the sections and compared diagrams made from one or two of every five sections to diagrams made from all of the sections. We found that, except for the density of the dots, the spatial distribution patterns seemed to be the same. Therefore, we used diagrams made from one of every five sections.

To allow comparison, all diagrams were simultaneously scaled along the rostral–caudal and dorsal–ventral axes so that they had the same rostral–caudal length. The diagrams were then corrected for differences in the angles of brain sectioning according to the locations of dorsal and ventral landmarks in each brain: the beginning and the joining of the left and right lateral ventricles (dorsal landmarks) and the start and end of the olfactory tubercle (ventral landmarks).

In mice exposed to distilled water or DMSO, there were some c-Fos$^+$ cells in the APC (Fig. 6, which is published as supporting information on the PNAS web site). Among three animals (six cortices), the total number of labeled cells per cortex ranged from 5 to 220, averaging 159 ± 50 for DMSO and 110 ± 74 for water (versus 84 ± 78 for air alone). In marked contrast to neurons activated by odorants, the locations of these cells varied widely among individuals.

Computational Analysis. The graphical data in Figs. 2, 3*A*, and 5*A* were transformed into quantitative data by superimposing a grid of 98 boxes on each graph and recording the number of cells in each box. Statistical analysis was performed by using R-PACKAGE (47). The basis for the analysis was a matrix of odorants versus activity patterns. In this matrix, the odorant stimuli were viewed as vector variables that were determined by activity patterns represented by the number and distribution of c-Fos$^+$ cells. Hierarchical clustering was performed with the average linkage method (47, 48).

Results

Spatial Representations of Odors in the OC. To investigate odor responses in the mouse OC, individual mice were placed in an isolated chamber suffused with charcoal-filtered air for 16 h, exposed briefly to an odorant, and then left in filtered air for an
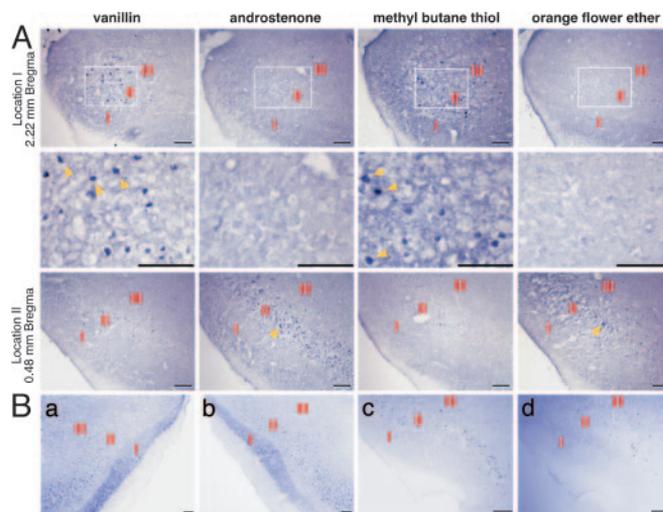

Fig. 1. Different cortical locations respond to different combinations of odorants. (*A*) c-Fos labeling in coronal sections from two APC locations after exposure to four different odorants. Images in the *Middle* are enlarged versions of the boxed areas seen in the *Top*. The distances of the APC locations from an anatomical landmark (Bregma) are shown. The layers of the OC are indicated by red Roman numerals. Yellow arrowheads point to c-Fos$^+$ neurons. Sparse c-Fos$^+$ neurons are seen in response to four odorants. The two locations responded to different odorants. (Scale bars, 100 μm.) (*B*) c-Fos$^+$ neurons are seen at the same APC location in coronal sections from the two hemispheres of one animal exposed to ethyl butyrate (*Ba* and *Bb*) and from two individuals exposed to methyl butane thiol (*Bc* and *Bd*). (Scale bar, 100 μm.)

additional hour to allow accumulation of c-Fos protein. Low concentrations of odorants were used to simulate what might be encountered in the natural environment. Brain sections from each animal were subsequently immunostained with antibodies against c-Fos and analyzed.

In initial experiments, we examined cortical responses to a number of odorants with varied structures. Fig. 1*A* shows two APC locations in mice exposed to four different odorants. c-Fos$^+$ neurons are localized in cortical layers II and III. This result is consistent with previous studies showing that, in the APC, odorants induce c-Fos predominantly or exclusively in layer II/III pyramidal neurons that receive direct excitatory input from the OB (49). In Fig. 1*A*, each APC location shows scattered c-Fos$^+$ neurons in response to two of the four odorants, but the stimulatory odorants differ for the two locations. These results indicate that one cortical location can respond to multiple odorants, but that different locations can respond to different combinations of odorants.

To examine the patterning of odorant responses across the entire APC, we constructed the composite diagrams shown in Fig. 2. Each diagram shows the positions of c-Fos$^+$ neurons in every fifth section (every 70 μm) through the APC and thus allows visualization of c-Fos labeling along the anterior-posterior and dorsal-ventral axes throughout the APC.

Fig. 2 shows composite diagrams of c-Fos$^+$ neurons in the APC of mice exposed to twelve different odorants. These data make three important points. First, each odorant stimulates c-Fos expression in a subset of neurons that are sparsely but unevenly distributed over a large area, the size of which varies among odorants. Second, different odorants stimulate different response patterns. And, finally, the response patterns for different odorants partially overlap. These results indicate that odor representations in the APC are sparse, distinct, and multiplexed. The identities of different odorants are mapped onto the APC in a complex, partially overlapping manner.
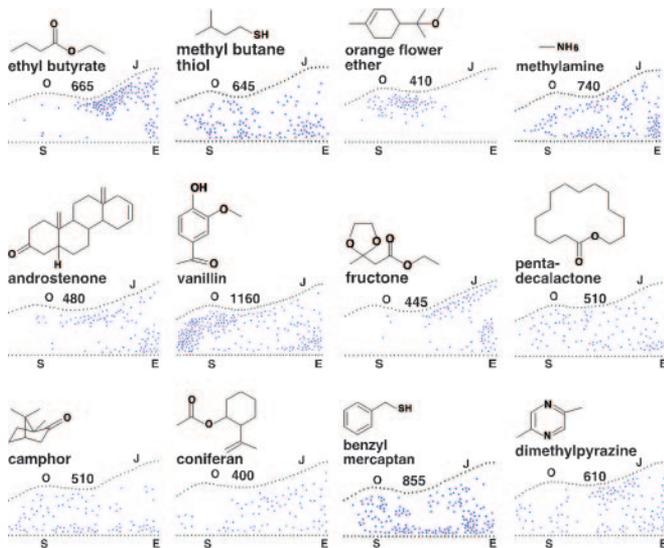
NEUROSCIENCE

Fig. 2. Different odorants elicit different response patterns. Patterns of c-Fos⁺ neurons across the full extent of the APC in response to twelve odorants. Each diagram shows the dorsal–ventral location of each c-Fos⁺ neuron (blue dot) in every fifth 14-μm coronal section along the anterior-posterior length of the APC. Dorsal is at the top and anterior on the left. Black dots indicate the dorsal and ventral limits of the APC in individual sections, with ventral limits placed on a horizontal line. The extrapolated number of c-Fos⁺ neurons in the entire APC (five times the number indicated by blue dots) is shown above each diagram. Locations of dorsal and ventral anatomical landmarks are indicated: S, start of olfactory tubercle; O, initial opening of lateral ventricle; J, joining of left and right lateral ventricles; E, end of olfactory tubercle. Odorant names and structures are shown above each diagram.

Cortical Representations Are Similar Among Individuals. We next compared the odor response patterns of different animals. In these experiments, we analyzed c-Fos expression in response to each of four odorants in the left and right brains of three mice. With each odorant, the patterns of labeled neurons were similar among individuals as well as in the two hemispheres (Fig. 3A). Examples of odor response similarities in single tissue sections from different cortices are shown in Fig. 1B. Control animals exposed to diluent alone (water or DMSO) had fewer c-Fos⁺ cells, and the locations of those cells varied widely among individuals (Fig. 6).

To analyze the odorant response patterns further, we superimposed a 292-box grid on each odor response diagram, marked each box that contained two or more labeled cells (in unextrapolated data from one in five tissue sections)(Fig. 3B), and then constructed a summary diagram (Fig. 3C), which shows boxes marked in three or more of the four cortices shown for each odorant. The marked diagrams in Fig. 3B emphasize the similarities in response patterns in different cortices. The summary diagrams in Fig. 3C further suggest that there are "hot spots" of activation for each odorant, regions of the APC that usually or always respond to that odorant. These hot spots are clearly different for the different odorants. Together, these studies indicate that odors are mapped onto the cortex in a related manner in different individuals and in the left and right brain.

Although similar, the patterns of c-Fos labeling in different cortices were not identical (Fig. 3 A and B). This variability could be inherent to the cortex, or, alternatively, it could result from differing input from the OB. To investigate the latter possibility, we used c-Fos induction in periglomerular cells as a reporter of glomerular activation in the corresponding OBs (23). The number of c-Fos⁺ neurons in the APC was roughly correlated with the number of activated glomeruli in the input OB. For one
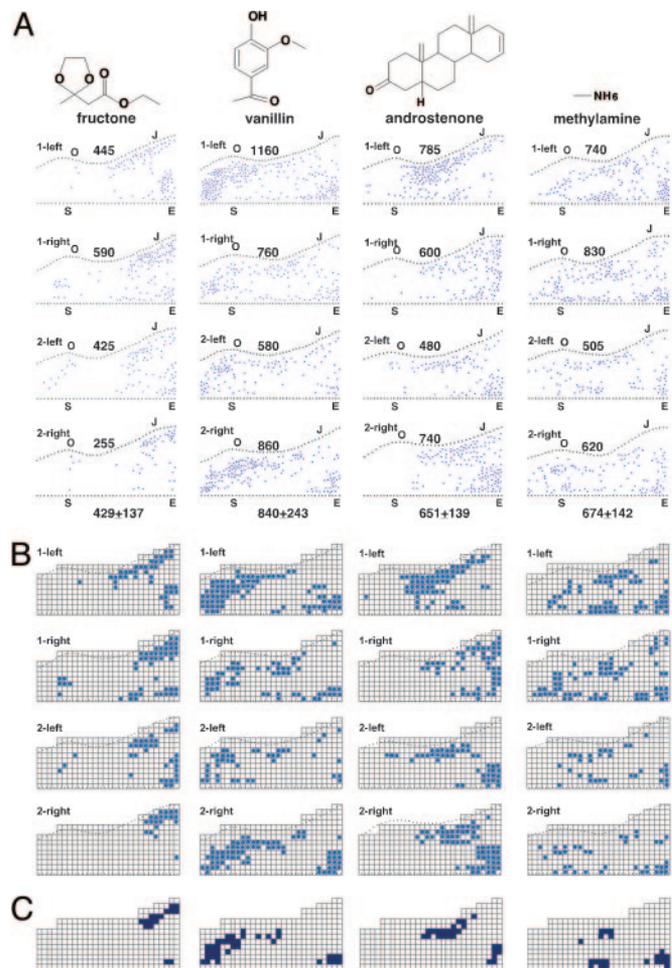

Fig. 3. Cortical odor response patterns are similar among individuals. (*A*) Diagrams show the locations of c-Fos⁺ neurons in the left and right APC of two mice for each of the odorants indicated, and the number of c-Fos⁺ neurons in each cortex (see Fig. 2 legend). Different animals exposed to the same odorant are specified by numbers (either 1 or 2). The two hemispheres are indicated (left or right). Below the diagram for each odorant is shown the average number of c-Fos⁺ neurons per cortex ± SD. The four odorants activated different, but partially overlapping, patterns of neurons, which are similar in the two hemispheres and in different individuals. (*B*) A 292-box grid was superimposed on each diagram in *A*, and each box containing two or more c-Fos⁺ neurons was marked in blue to clarify the patterns elicited by each odorant. Because the APC is 10.5 mm² (28), each box represents an ≈190-um² segment of the APC. (*C*) Colored boxes are those that are marked in *B* in at least three of the four APC diagrams for each odorant. The colored boxes represent hot spots of activation for each odorant. They are distinct, but partially overlapping, for the four odorants.

odorant (methylamine), cortices with 335, 495, 505, 620, 740, and 830 c-Fos⁺ neurons received input from bulbs containing 8, 8, 9, 12, 15, and 22 c-Fos⁺ glomeruli, respectively. This finding suggests that at least some of the variation in APC responses derives from variability in sensory input from the OB. Other potential sources of variability are intrinsic variation in odor response patterns among cortices and technical difficulties inherent to the comparison of brains from different individuals.

To further compare odor representations in different cortices, we performed computational analyses (47, 48). Using data from gridded diagrams of c-Fos labeling, we conducted a hierarchical cluster analysis to assess pattern similarities (Fig. 4). Almost invariably, activity patterns elicited by an odorant in different cortices were grouped, emphasizing their similarity.
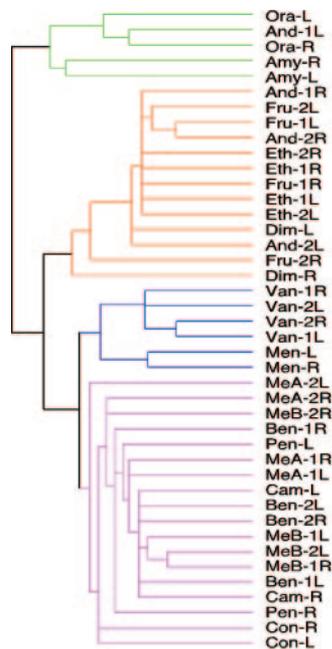
Fig. 4. Computational analysis of cortical odor representations. Shown is a hierarchical cluster analysis of c-Fos labeling patterns. Cortical patterns are grouped according to similarity (average linkage). Pattern similarity is expressed as cluster distance. The 42 cortices analyzed form four large groups. Patterns elicited by the same odorant in different individuals and the two hemispheres are almost invariably in the same group. Odorants are as follows: And, androstenone; Amy, amyl cinnamic aldehyde; Ben, benzyl mercaptan; Cam, camphor; Con, coniferan; Dim, dimethylpyrazine; Eth, ethyl butyrate; Fru, fructone; Men, menthol; MeA, methylamine; MeB, methyl butane thiol; Ora, orange flower ether; Pen, pentadecalactone; and Van, vanillin. Different mice exposed to the same odorant are indicated by numbers. L, left hemisphere; R, right hemisphere.

Related Odorants with Similar Representations. To investigate potential relationships between cortical representations and odorant structures, we compared the patterns of c-Fos expression stimulated by structurally related odorants. We tested two pairs of related odorants: two esters, fructone and ethyl butyrate, and two thiols, methyl butane thiol and benzyl mercaptan (Fig. 5A).

These experiments showed that odorants with related structures can have very similar cortical representations. This finding was true not only for the two esters, which have highly related structures, but also for the two thiols, which have only a thiol group in common (Fig. 5A). The high degree of relatedness in the representations of the related odorants is further emphasized by similarities in their activation hot spots (Fig. 5A) as well as their high similarity according to hierarchical cluster analyses (Fig. 4).

Odorant Concentration Affects Cortical Representations. We next asked whether the concentration of an odorant affects its cortical representation. In these experiments, odorants were tested at concentrations differing by 10-fold.

A 10-fold increase in concentration had three discernible effects (Fig. 5B). First, it increased the number of c-Fos$^+$ APC neurons ($\approx$4-fold for methylamine and 2-fold for ethyl butyrate). Second, it caused an expansion of the odorant's spatial representation across the cortical sheet and, in some cases, the appearance of new regions of activation. Third, it increased the density of c-Fos$^+$ neurons at some locations. The maximum density of labeled neurons per 190-μm^2 cortical segment (as indicated by the number of labeled cells per box in gridded data similar to those in Fig. 3B) increased 2.3-fold for methylamine and 1.5-fold for ethyl butyrate. Similar increases were seen for

methyl butane thiol (1.5-fold) and camphor (2.5-fold), but not for androstenone (data not shown).

By using extremely high concentrations of odorants, the density of c-Fos$^+$ neurons in a hot spot area (Fig. 5Ca) approached that of pyramidal neurons labeled by a transneuronal tracer expressed in all OE neurons (50) (Fig. 5Cb). This result suggests that most or all APC pyramidal neurons can express c-Fos in response to sensory input.

Discussion

Here, we investigated how odors are represented in the OC. We first exposed mice to diverse odorants and then used antibodies against c-Fos to analyze resulting patterns of neuronal activation in the anterior piriform cortex. The results of these experiments provide initial insight into how odors are spatially represented in the cortex. They reveal that odor representations are dramatically transformed when sensory signals are transmitted from the olfactory bulb to the piriform cortex.

These studies show that, in the APC, each odorant is represented by a small subset of cortical neurons that are highly distributed across the cortical sheet. The area over which these neurons are distributed varies among odorants. Neurons activated by some odorants are scattered over much of the APC whereas neurons activated by other odorants are confined to smaller regions. The neurons are unevenly distributed, with some regions containing higher densities of activated neurons than others.

Previous studies indicate that each odorant is detected by a combination of different ORs (14, 20, 21) and that input from one OR is targeted to neurons distributed over $\approx$5% of the APC surface (28). In the present studies, the percentage of the APC surface area containing c-Fos-labeled neurons varied among odorants, but ranged from $\approx$19% to 27% for four odorants tested in multiple individuals (based on the percentage of boxes containing two or more c-Fos$^+$ neurons in gridded data in Fig. 3B). This finding indicates that inputs from different ORs that detect the same odorant are not all targeted to the same APC locations. However, it does not exclude the possibility that inputs from some of those ORs are mapped onto the same, or partially overlapping, locations.

A second important finding of these studies is that odorants elicit conserved response patterns in the APC. The patterns are similar in different individuals as well as in the two hemispheres. This finding is consistent with the stereotyped patterning of OR inputs previously seen in the APC in genetic tracing studies (28). However, unlike patterns of OR inputs in the APC, which are nearly identical among individuals, slight variations are seen in both the number and patterning of odorant-responsive neurons in different cortices. Some of this variation seems to be due to variability in sensory input from the olfactory bulb, which could, in turn, be due to alternating respiration through the two nostrils (51, 52). Another potential source of variability might be experience-dependent effects on odor response patterns.

These studies demonstrate that different odorants can elicit distinctly different patterns of activity in the APC. The only previous study to examine odor-induced activation patterns in the APC found similar patterns of c-Fos activation for different odorants in the rat, but tested a smaller number and diversity of odorants (49). In the present studies, related patterns were elicited by some odorants, but not others. Importantly, however, the patterns stimulated by different odorants partially overlapped. These findings indicate that sensory information is mapped onto the cortex in a complex, multiplexed fashion. There are no discrete odor maps. Rather, the identities of different odorants are represented by subsets of neurons in extensively overlapping spatial arrays.

The present studies further show that odor response patterns in the cortex are altered by changes in odorant concentration. With a 10-fold increase in odorant concentration, the odorant's representation in the APC typically expanded to include a larger number of neurons that were increased in density and extended
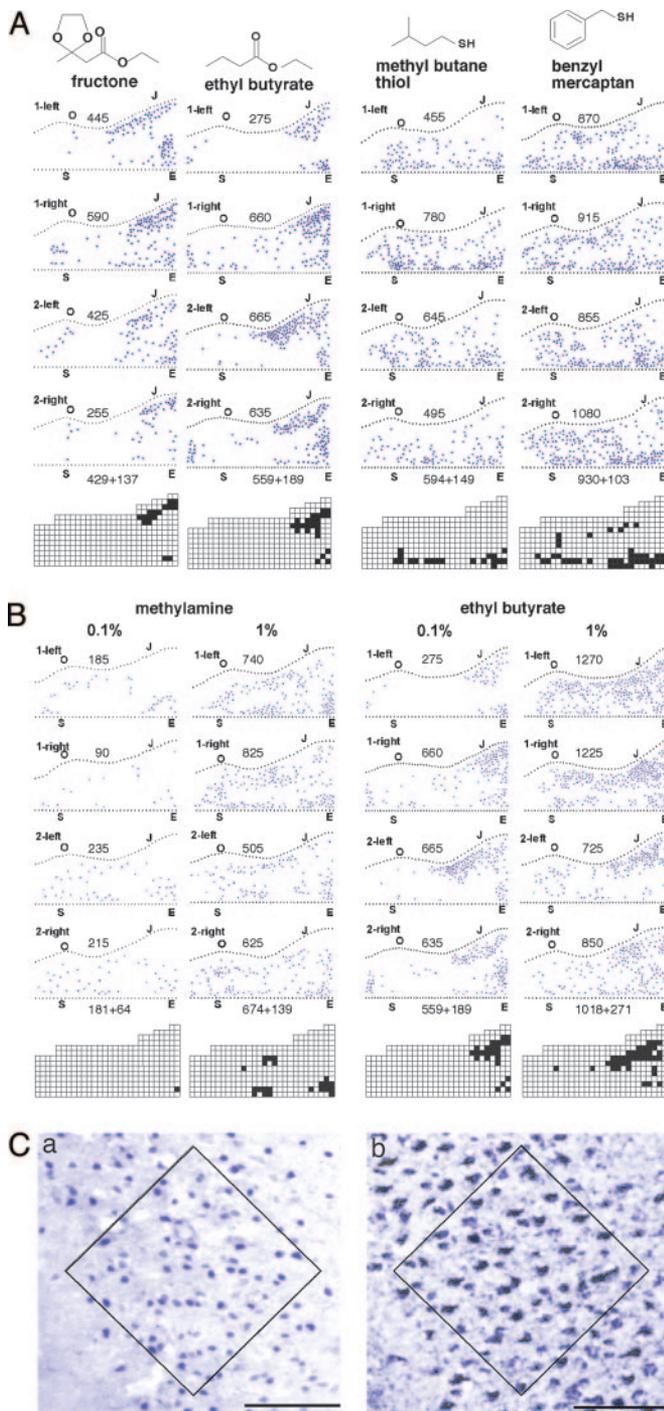
Fig. 5. Effects of odorant structure and concentration on cortical responses. (*A*) Diagrams (see Fig. 2 legend) show the patterns of c-Fos-labeled neurons in the left and right APC of two mice after exposure to two pairs of related odorants: two esters (fructone and ethyl butyrate) and two thiols (methyl butane thiol and benzyl mercaptan). The number of c-Fos$^+$ neurons in the entire APC is shown above each diagram; the number below the 4th diagram is the average $\pm$ SD. Activation hot spots are shown below for each odorant. The related odorants elicited highly related response patterns in the APC. (*B*) Diagrams show the locations of c-Fos$^+$ neurons in the APC after exposure to different concentrations of methylamine or ethyl butyrate. The total number of c-Fos$^+$ neurons in each cortex is shown above its corresponding diagram, and the average $\pm$ SD is shown below for each odorant and odorant concentration. A 10-fold rise in odorant concentration increased the number of c-Fos$^+$ neurons and expanded the spatial representation for each odorant. (*C*) High magnification photographs of one region of the APC show pyramidal neurons labeled for c-Fos protein in a mouse exposed to an unnaturally high

over a larger proportion of the APC. These changes presumably reflect effects of increased odorant concentration on the olfactory epithelium and bulb, including the recruitment of additional ORs (14), sensory neurons (22), and bulb glomeruli (24, 26, 27) into the odor response as well as increases in the firing of sensory neurons (53) and bulb projection neurons (54).

Is there any logic to the way that olfactory information is represented in the cortex? These studies show that structurally related odorants can elicit highly related patterns in the APC. One possible explanation for this result is that the related odorants are detected by many of the same ORs. Another possibility is that information is mapped onto the cortex according to individual structural features of odorants. Future studies of cortical inputs from ORs that recognize the same odorant feature should provide insight into whether there is such a logic in the organization of information in the APC.

Even though each odorant is detected by a combination of ORs, the number (and density) of c-Fos$^+$ neurons seen in the APC (often $\approx$500–1,000 cells per APC) (Figs. 2, 3*A*, and 5*A*) after exposure to a low concentration of an odorant was lower than the number that receive input from one OR ($\approx$5,000 cells per APC) (28). One possible explanation for this difference is that c-Fos is not detected in neurons that are only weakly activated by an odorant. However, electrophysiological recordings similarly indicate that single odorants activate only a small percentage of neurons in the piriform cortex (32, 33, 35, 36, 38), arguing against this possibility. Another potential explanation for the observed difference between OR inputs and neuronal activation is that intrinsic inhibitory circuits shape odor responses in the cortex and eliminate responses to a particular odorant by many neurons that receive input from a given OR. Yet another possibility is that cortical neurons are activated predominantly by combinatorial OR inputs. In this scenario, cortical neurons would function as "coincidence detectors" that are activated only by correlated signals derived from different ORs. In this model, two odorants detected by an OR, OR-X, but recognized by different combinations of ORs, might activate different subsets of neurons because those subsets receive input from different combinations of ORs.

In sensory systems, stimuli in the external world are deconstructed and then reconstructed in the brain to create diverse perceptions (1). In the olfactory system, the stimuli are a multitude of structurally diverse odorants (55). The serial transformations of olfactory input that occur as it travels through different structures in the olfactory pathway are reminiscent of other sensory systems. In the visual system, the deconstructed features of visual stimuli are combined in single neurons in an increasingly complex fashion as information travels from the retina to the thalamus to primary visual cortex and then to higher visual cortical areas (56). In the olfactory system, 1,000 different ORs are used in different combinations to detect different odorants and encode their identities (14, 20, 21). The odorant stimulus is thus deconstructed into a combination of ORs, that, by analogy with the visual system, might be thought of as encoding different features of the stimulus. Although inputs from different ORs are segregated in different neurons in the olfactory epithelium and bulb (14–20), single cortical neurons are likely to receive signals derived from combinations of ORs (28). Based on the findings presented here, we speculate that neurons in the OC require combinatorial OR signals for activation. This design could represent a first step in the reconstruc-

concentration of methyl butane thiol (*Ca*) or for a genetic transneuronal tracer produced in all olfactory sensory neurons in a transgenic mouse (*Cb*) (50). The boxed regions contain 56 c-Fos$^+$ cells (nuclei) in *Ca*, and 55 tracer-labeled cells in *Cb*, indicating that most or all pyramidal neurons in the boxed area can express c-Fos in response to an odorant. (Scale bar, 100 μm.)

tion of the odorant stimulus by the integration of its deconstructed features in single neurons.

1. Kandel, E. R., Schwartz, J. H. & Jessell, T. M. (2000) *Principles of Neural Science* (McGraw–Hill, New York).
2. Scott, J. W. (1986) *Experientia* **42,** 223–232.
3. Price, J. L. (1987) in *Neurobiology of Taste and Smell*, eds. Finger, T. E. & Silver, W. L. (Wiley, New York), pp. 179–203.
4. Shipley, M. T. & Ennis, M. (1996) *J. Neurobiol.* **30,** 123–176.
5. Neville, K. R. & Haberly, L. B. (2004) in *The Synaptic Organization of the Brain*, ed. Shepherd, G. M. (Oxford Univ. Press, New York), pp. 415–454.
6. Buck, L. & Axel, R. (1991) *Cell* **65,** 175–187.
7. Zhao, H., Ivic, L., Otaki, J. M., Hashimoto, M., Mikoshiba, K. & Firestein, S. (1998) *Science* **279,** 237–242.
8. Araneda, R. C., Kini, A. D. & Firestein, S. (2000) *Nat. Neurosci.* **3,** 1248–1255.
9. Firestein, S. (2001) *Nature* **413,** 211–218.
10. Zhang, X. & Firestein, S. (2002) *Nat. Neurosci.* **5,** 124–133.
11. Young, J. M. & Trask, B. J. (2002) *Hum. Mol. Genet.* **11,** 1153–1160.
12. Godfrey, P. A., Malnic, B. & Buck, L. B. (2004) *Proc. Natl. Acad. Sci. USA* **101,** 2156–2161.
13. Mombaerts, P. (2004) *Nat. Rev. Neurosci.* **5,** 263–278.
14. Malnic, B., Hirono, J., Sato, T. & Buck, L. B. (1999) *Cell* **96,** 713–723.
15. Ressler, K. J., Sullivan, S. L. & Buck, L. B. (1993) *Cell* **73,** 597–609.
16. Vassar, R., Ngai, J. & Axel, R. (1993) *Cell* **74,** 309–318.
17. Ressler, K. J., Sullivan, S. L. & Buck, L. B. (1994) *Cell* **79,** 1245–1255.
18. Vassar, R., Chao, S. K., Sitcheran, R., Nunez, J. M., Vosshall, L. B. & Axel, R. (1994) *Cell* **79,** 981–991.
19. Mombaerts, P., Wang, F., Dulac, C., Chao, S. K., Nemes, A., Mendelsohn, M., Edmondson, J. & Axel, R. (1996) *Cell* **87,** 675–686.
20. Buck, L. B. (2000) *Cell* **100,** 611–618.
21. Kajiya, K., Inaki, K., Tanaka, M., Haga, T., Kataoka, H. & Touhara, K. (2001) *J. Neurosci.* **21,** 6018–6025.
22. Ma, M. & Shepherd, G. M. (2000) *Proc. Natl. Acad. Sci. USA* **97,** 12869–12874.
23. Guthrie, K. M. & Gall, C. M. (1995) *Chem. Senses* **20,** 271–282.
24. Rubin, B. D. & Katz, L. C. (1999) *Neuron* **23,** 499–511.
25. Uchida, N., Takahashi, Y. K., Tanifuji, M. & Mori, K. (2000) *Nat. Neurosci.* **3,** 1035–1043.
26. Johnson, B. A. & Leon, M. (2000) *J. Comp. Neurol.* **422,** 496–509.
27. Fried, H. U., Fuss, S. H. & Korsching, S. I. (2002) *Proc. Natl. Acad. Sci. USA* **99,** 3222–3227.
28. Zou, Z., Horowitz, L. F., Montmayeur, J. P., Snapper, S. & Buck, L. B. (2001) *Nature* **414,** 173–179.
29. Mori, K., Nagao, H. & Yoshihara, Y. (1999) *Science* **286,** 711–715.
30. Shepherd, G. M., Chen, W. R. & Greer, C. A. (2004) in *The Synaptic Organization of the Brain*, ed. Shepherd, G. M. (Oxford Univ. Press, New York), pp. 165–216.
31. Scott, J. W., Wellis, D. P., Riggott, M. J. & Buonviso, N. (1993) *Microsc. Res. Tech.* **24,** 142–156.
32. Haberly, L. B. (1969) *Brain Res.* **12,** 481–484.
33. Tanabe, T., Iino, M. & Takagi, S. F. (1975) *J. Neurophysiol.* **38,** 1284–1296.
34. Nemitz, J. W. & Goldberg, S. J. (1983) *J. Neurophysiol.* **49,** 188–203.
35. McCollum, J., Larson, J., Otto, T., Schottler, F., Granger, R. & Lynch, G. (1991) *J. Cognit. Neurosci.* **3,** 293–299.
36. Schoenbaum, G. & Eichenbaum, H. (1995) *J. Neurophysiol.* **74,** 733–750.
37. Wilson, D. A. (2000) *J. Neurophysiol.* **83,** 139–145.
38. Litaudon, P., Amat, C., Bertrand, B., Vigouroux, M. & Buonviso, N. (2003) *Eur. J. Neurosci.* **17,** 2457–2461.
39. Sheng, M. & Greenberg, M. E. (1990) *Neuron* **4,** 477–485.
40. Morgan, J. I. & Curran, T. (1991) *Annu. Rev. Neurosci.* **14,** 421–451.
41. Herrera, D. G. & Robertson, H. A. (1996) *Prog. Neurobiol.* **50,** 83–107.
42. West, A. E., Chen, W. G., Dalva, M. B., Dolmetsch, R. E., Kornhauser, J. M., Shaywitz, A. J., Takasu, M. A., Tao, X. & Greenberg, M. E. (2001) *Proc. Natl. Acad. Sci. USA* **98,** 11024–11031.
43. Scheich, H. & Zuschratter, W. (1995) *Behav. Brain Res.* **66,** 195–205.
44. Montero, V. M. & Jian, S. (1995) *Brain Res.* **690,** 189–199.
45. Filipkowski, R. K., Rydz, M., Berdel, B., Morys, J. & Kaczmarek, L. (2000) *Learn. Mem.* **7,** 116–122.
46. Melzer, P. & Steiner, H. (1997) *J. Comp. Neurol.* **380,** 145–153.
47. Johnson, D. E. (1998) *Applied Multivariate Methods for Data Analysts* (Duxbury, Pacific Grove, CA).
48. Friedrich, R. W. & Korsching, S. I. (1997) *Neuron* **18,** 737–752.
49. Illig, K. R. & Haberly, L. B. (2003) *J. Comp. Neurol.* **457,** 361–373.
50. Horowitz, L. F., Montmayeur, J. P., Echelard, Y. & Buck, L. B. (1999) *Proc. Natl. Acad. Sci. USA* **96,** 3194–3199.
51. Werntz, D. A., Bickford, R. G., Bloom, F. E. & Shannahoff-Khalsa, D. S. (1983) *Hum. Neurobiol.* **2,** 39–43.
52. Werntz, D. A., Bickford, R. G. & Shannahoff-Khalsa, D. (1987) *Hum. Neurobiol.* **6,** 165–171.
53. Getchell, T. V. & Shepherd, G. M. (1978) *J. Physiol.* **282,** 521–540.
54. Cang, J. & Isaacson, J. (2003) *J. Neurosci.* **23,** 4108–4116.
55. Amoore, J. E. (1970) *Molecular Basis of Odor* (Thomas, Springfield, IL).
56. Hubel, D. (1988) *Eye, Brain, and Vision* (Scientific American Library, New York).

NEUROSCIENCE